INNOVATION FOREVER
Open Access

Innovation Discovery

ISSN 2959-5150 (Online)

Short Communication

Functionalization of Gold Nanoparticles with Polymer Coatings in One Pot Reaction for the Detection of Explosives

Christopher Zaleski[1*], Volodymyr Chegel[2], Andrii Lopatynskyi[2], Vitalii Lytvyn[2], Michael Whitcombe[1], Alvaro Garcia Cruz[1], Elena Piletska[1], Sergey Piletsky[1]

[1]*Department of Chemistry, University of Leicester, Leicester, UK*
[2]*V.E.Lashkaryov Institute of Semiconductor Physics, National Academy of Science of Ukraine, Kyiv, Ukraine*

[*]***Correspondence to: Christopher Zaleski, PhD, Research Fellow,*** *Department of Chemistry, University of Leicester, University Road, Leicester, LE1 7RH, United Kingdom; Email: cz155@le.ac.uk*

Abstract

Growing safety and environmental threats increase the demand for new, affordable and durable sensors. This in turn necessitates the development of novel detection techniques. To address this need, much of research focus has been centred on molecularly imprinted polymers (MIPs) which are an emerging class of sensors with many possible applications. Our group has developed MIPs based on surface functionalized composite gold- polymer nanoparticles serving as sensors for explosive analogues. These novel materials were synthesized in one-pot reaction combining gold reduction and target imprinted polymer shell formation. Initially, gold nanoparticles have been formed during ketone catalysed reduction. Newly formed surfaces of gold nanoparticles acted as catalytic sites for hydroxyl radical formation. Formation of the imprinted polymer shell on the surfaces of gold nanoparticles was then catalysed by hydroxyl radicals. As a result of this, composite nanoparticles composed of gold core and polymer envelope were formed with >70% Au atom economy. These composite gold-polymer nanoparticles were used in localized surface plasmon resonance (LSPR) sensors for the detection of an explosive analogue – o-nitrophenol which is an analogue for a well-known explosive – trinitrotoluene. Finally, development of a prototype portable LSPR sensor has also been reported and this prototype device was able to detect target molecule in field applications, with high sensitivity in both vapour and liquid phases.

Keywords: nanoparticles, localised surface plasmon resonator, femtomolar, explosives

Received: December 3, 2025
Revised: May 1, 2026
Accepted: May 7, 2026
Published: May 25, 2026

Copyright © 2026 The Author(s). Published by Innovation Forever Publishing Group Limited. This open-access article is licensed under a Creative Commons Attribution 4.0 International License (https://creativecommons.org/licenses/by/4.0), which permits unrestricted use, sharing, adaptation, distribution, and reproduction in any medium, provided the original work is properly cited.

Citation: Zaleski C, Chegel V, Lopatynsky A, Lytvyn V, Whitcombe M, Garcia Cruz A, Piletska E, Piletsky S. Functionalization of Gold Nanoparticles with Polymer Coatings in One Pot Reaction for the Detection of Explosives. *Innov Discov*, 2026; 3(2): 7.

1 INTRODUCTION

Demands of global security necessitate development of new tools for sensitive and selective detection of explosives. Particular emphasis has been placed on the detection of explosives in vapour phase as this is a necessary approach for the detection of landmines and unexploded ordnance, which can represent significant danger even after a century had passed from the military conflict[1-3]. Vast majority of efforts have been centred on traditional, well-established methods of analytical chemistry[4,5]. A particular emphasis in developing explosives sensors has been made on mass spectrometry. Application of this technology resulted in the development of portable mass spectrometers which offer excellent reliability, versatility and nanogram level limits-of-detection (LODs) in both qualitative[6] and quantitative modes[7-12] but are often prohibitively expensive. Microgravimetry is another method that has found its way into the explosives detection[13,14]. A small number of QCM based explosives detectors has been reported with LOD at high nanogram level. Field applications are however questionable as this type of detector often suffers from being non-specific[15]. Application of Raman spectroscopy for the detection of explosives has also been very widely explored[16-19]. As a result of this, several Raman-based devices have been introduced to the market[20-22]. Chemiluminescence and fluorescence are other phenomena which are frequently applied for the detection of explosives with several types of detectors already developed[23-25]. Unfortunately, all

of these sensors suffer from drawbacks such as high costs, inability to operate in autonomous regime, high sensitivity to environmental changes and exposure to interferences as well as slow turnover which affects the number of samples that can be analyzed.

To answer the growing demand which necessitates development of new, more affordable and versatile detectors we present a novel approach based on molecularly imprinted polymers (MIPs) combined with localized surface plasmon resonance (LSPR). Sensors based on MIPs are usually classified as polymer analogues of the biological antibody–antigen systems[26,27]. Similarly to antibodies, they use a "lock and key" mechanism to selectively bind the target molecule. Binding cavities are formed within MIP when target molecule is used as a template during MIP synthesis. MIPs potentially offer the specificity and selectivity of the biological receptors with notable advantage of durability to environmental conditions while being a low-cost material[28,29]. MIPs are very robust and can be exploited at extreme environmental conditions while not having special storage requirements like biological antibodies. MIPs have excellent binding affinity to targets, typically reaching nanomolar limits of detection[30-33].

Detection of explosives using MIP based optical and electrochemical sensors has been reported previously, however the experimental set up reported was complex, expensive and not portable, thus limiting practical applications[34]. Nevertheless, the detection limit demonstrated by these sensors reached femtomolar levels needed for the detection of explosives in liquid and gas phases in field applications demonstrating MIPs potential as the detectors of explosives. MIP based SPR (Surface Plasmon Resonance) sensors for the detection of explosives were also reported[35,36]. The main issue with this approach was in poor reproducibility of the procedure for creating robust polymer layers fully integrated with gold nanoparticles affecting sensor performance. None of these approaches resulted in a practical device entering the market.

At the core of LSPR approach are gold nanoparticles which are prone to aggregation, and protective coatings composed of citric acid or other molecules are thus often used to prevent this. This approach unfortunately interferes with photopolymerization making it not feasible for coating nanomaterials which strongly absorb light (like AuNPs) thus preventing irradiation reaching all the particles in the bulk volume. It is known that Au, Pt, Pd and Ag nanoparticles possess catalytic activities which can be exploited for chemical activation of polymerisation process and therefore polymer shell formation[37]. In situ formation of metal nanoparticles coated with polymer is indeed possible and has been reported before[38]. In this work, noble metals ions were reduced to nanoparticles in redox-oxidation polymerisation with $HAuCl_4$. This process however is restricted to very specific class of monomers such as dopamine, aniline, phenols etc. that are prone to oxidative polymerisation. To overcome all the previous obstacles our team has developed a new one pot synthesis, where gold nanoparticles are formed in a monomer solution, working further as catalysts in reaction with hydrogen peroxide and monomers and leading to the formation of uniform polymer layer on the surface of newly formed gold-polymer nanoparticles. We then used thus formed Au-core MIPs (AuMIPs) as sensors for explosive analogues.

Our sensing approach relies on MIP enhanced LSPR detection. Similar approach of utilization of 3-D nanostructures in SPR spectroscopy has been reported by several groups before[39,40]. At the core of our experiments lies glass slide functionalised with gold nanoparticles, coated with thin film of AuMIPs. It has been anticipated that the composite nanoparticles reported in this work will reach femtomolar limits of detection comparable with results reported for the state-of-the-art LSPR while significantly reducing the cost and size of the equipment.

2 MATERIALS AND METHODS

2.1 Reagents

Acrylic acid, N-3-Aminopropyl methyl acrylamide, N-isopropyl acrylamide, N-tert-butyl acrylamide, N,N'-methylenebisacrylamide (MBAA), hydrogen peroxide 50% aqueous solution, o-nitrophenol, acetone, acetylacetone, N-(3-Dimethylaminopropyl)-N'-ethylcarbodiimide hydrochloride, N-Hydroxysuccinimide and mercaptoundecanoic acid were all purchased from Sigma Aldrich and used as received apart from the ketones which were premixed in a 2 acetylacetone/1 acetone volume ration as this has been found to be the most effective reducing agent for the formation of gold nanoparticles.

Dialysis tubing, Polypropylene solid-phase extraction tubes (60mL), polyethylene frits, disposable plastic syringes, syringe filter membrane 0.45 and 0.75µm, and UV-visible cuvettes were purchased from Sigma-Aldrich. Magnetic stirrer hotplates, Buchner filter flasks, Buchner filter cones, flat-bottomed glass vessels were purchased from Fisher Scientific. Glass vials and disposable plastic cuvettes were obtained from VWR International. Template molecule used was an explosive analogue (o – nitrophenol which is an analogue for trinitrotoluene). In order to ensure that a sufficient number of binding cavities has been formed during the polymerization process, ratio of template to monomer has been set as 1:10 by weight based on our previous research[41].

Au-MIPs were synthesized in the presence of the target molecule as follows: Step 1 was the preparation of the

Table 1. List of Reagents Used in Functionalization of Gold Nanoparticles with Polymer Coatings in One Pot Reaction

Reagent	Application	Concentration/Amount
N (3 aminopropyl) methylacrylamide hydrochloride	Monomer	0.34mM
N-isopropylacrylamide	Monomer	3.4mM
N-tert butylacrylamide	Monomer	2.36mM
Acrylic acid	Monomer	0.32mM
N, N – methylene bis acrylamide	Cross-linker	0.38mM
Chloroauric acid trihydrate	Au salt	0.0005mM
Hydrogen peroxide	Polymerization initiator	0.6 ml @ 50 %
Acetone	Reducing agent	0.167mL
Acetylacetone	Reducing agent	0.333mL
Ethanol	Solvent	N/A
HPLC water	Solvent	N/A
Phosphate saline buffer pH 7	Buffer	1 tablet
O-nitrophenol	Target substance	10mg
1-Ethyl-3-(3-dimethylaminopropyl) carbodiimide	AuMIP immobilization	15 mg
N-Hydroxy succinimide	AuMIP immobilization	10 mg
Mercaptoundecanoic acid	AuMIP immobilization	10 mg

monomeric mixture which was produced by adding N (3 aminopropyl) methylacrylamide hydrochloride (3mg, 0.34mM), N-isopropylacrylamide (19.5mg, 3.4mM), N-tert butylacrylamide (15mg, 2.36mM initially dissolved in 400µL of Ethanol), acrylic acid (22µL initially dissolved in 50µL of EtOH) and N, N – methylene bis acrylamide (wt. 3mg, 0.38mM) to 50mL of N_2 degassed (10 mins at 0.4Lmin^{-1} flow rate) 100mM phosphate saline buffer pH 7 (PBS). Step 2: Addition of 30µL of chloroauric acid trihydrate solution (6.6mg mL^{-1}). Step 3: Addition of target molecule (10mg of o-nitrophenol). Step 4: Polymerization initiation through the addition of 600µL of 50% hydrogen peroxide (H_2O_2) followed by an addition of 0.5mL of reducing agent (2:1 acetylacetone/acetone by volume) to the monomeric mixture. Both reagents were added all at once. Then, the mixture was deoxygenated using N_2 stream for 10 minutes and left to settle. Step 5: Purification against multiple changes of HPLC water using dialysis membranes with cut-off mass of 10kDa. The entire reaction and purification processes were conducted at a room temperature.

2.2 Material Characterization

Dynamic light scattering (DLS) experiments were performed using Zetasizer Nano (Nano-S) particle-size analyser from Malvern Instruments Ltd. (UK). LSPR analysis was performed using Nano SPR-103 spectrometer, (NanoSPR, Chicago, USA). TEM images were taken using a Philips CM20 transmission electron microscope. IR spectroscopy was preformed using Fourier Transformation Infra-Red (FTIR) Alpha II spectrometer, Bruker. Prior to infra-red spectroscopic and microscopic observations MIPs were freeze dried (Alpha 1 – 2 LD plus, CHRIST) and kept at room conditions with no appreciable degradation observed.

Immobilization of Au-MIPs on Au coated glass slides is described in Appendix Section 4. Images of AuMIPs immobilized on the surface of Au coated chips are shown in Figure S2. Afterwards immobilized AuMIPs were used for target detection. Measurements were performed at an ambient temperature of 20°C and air humidity of 40%.

2.3 Detection of Explosive Analogue

In order to simulate trace amounts of explosives to be detected, the following protocol to obtain low amounts of explosive analogue to be used in sensing was developed. Solid explosive analogue (e.g., o – nitrophenol) was dissolved in 2-propanol and then successively diluted to obtain a set of solutions with explosive analogue concentrations down to 100fg/mL. 10µL aliquots of solutions in a selected concentration range were then transferred to spectrophotometric cuvettes (with a volume of 4.5cm^3) and allowed to dry completely to form a thin solid coating on the bottom and on the walls of the cuvettes, and then the cuvettes were sealed with a paraffin film. This method easily allowed obtaining the quantified amounts of explosive analogue in the femtogram – microgram range, with lower part of this range corresponding to picomolar and femtomolar levels of respective substance. Storing the prepared samples in sealed cuvettes produced a stable atmosphere of explosive analogue vapors of different concentration, which was then used to assess the concentration-dependent response of the developed 2-channel photometric sensor for explosives detection.

3 RESULTS AND DISCUSSION

3.1 Au-MIP Nanoparticles

Au-MIP nanoparticles were prepared by an in-situ

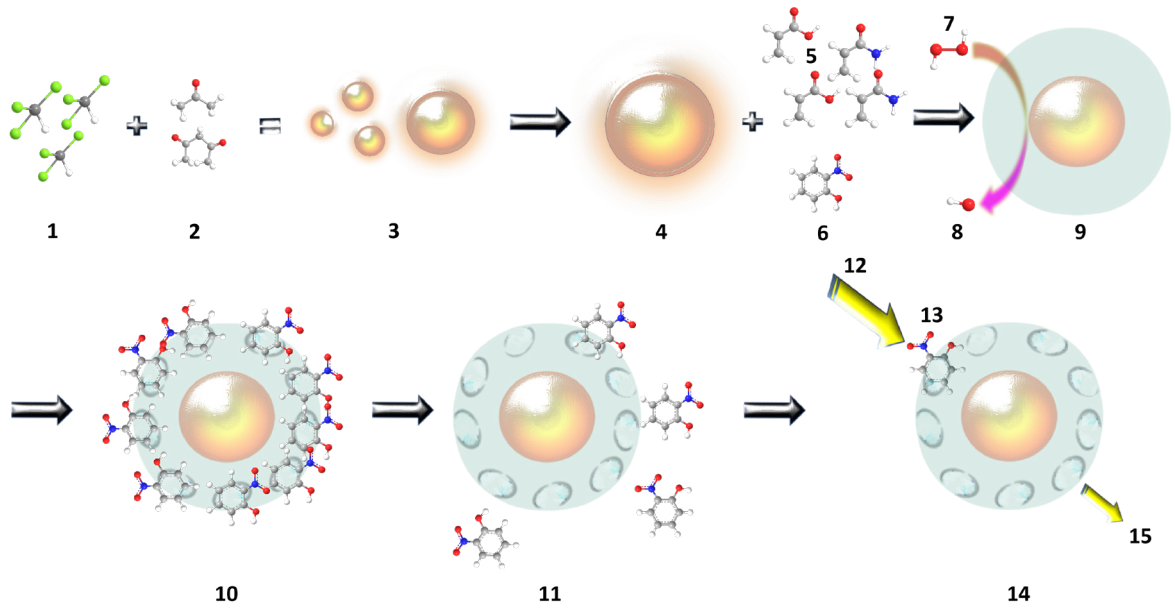


Figure 1. Schematic Representation of One-pot AuMIPs Synthesis. 1 – HAuCl3+ ions, 2 – acetone and acetylacetone molecules, 3 – formation of AuNPs, 4 – fully formed AuNP, 5 – monomers in MIP polymerization, 6 – target molecule (o-nitrophenol), 7 – hydrogen peroxide, 8 *OH radical, 9 – coating of AuNP with a polymer layer in *OH radical initiated polymerization, 10 – fully formed AuMIP with target molecules present in binding cavities, 11 – removal of target molecules in post-polymerization purification, 12 – incident beam of light during LSPR analysis, 13 – target molecule bound to an AuMIP, 14 – AuMIP with target-specific binding sites, 15 – LSPR absorbance directly proportional to the target molecule concentration.

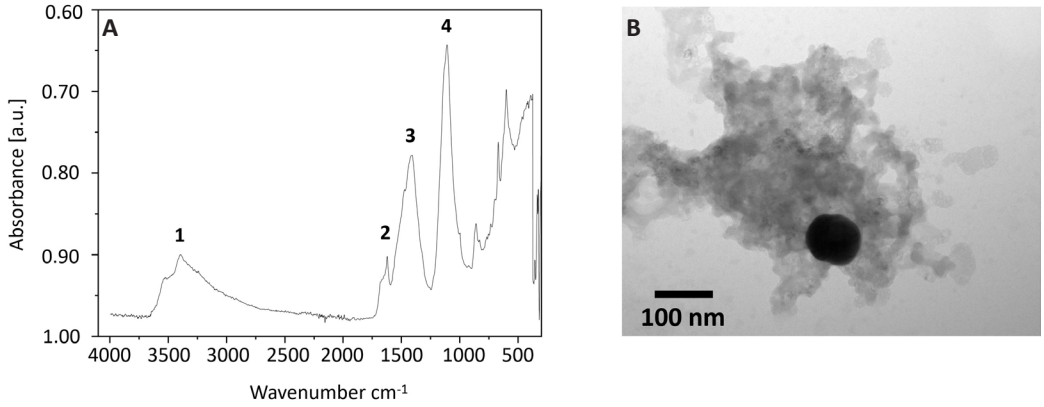


Figure 2. Characterization of AuMIPs. A: FTIR Spectroscopy of AuMIPs, 1 – NH group, 2 – C=O group, 3 – CH group, 4 – C=O group. B: TEM images of Au-MIPs.

polymerization method which relies on rapid formation of high number of AuNPs followed by an immediate formation of *OH radicals through decomposition of H_2O_2 on AuNPs surfaces. Thus, formed hydroxyl radicals initiate rapid formation of polyacrylamide shells on the surface of AuNPs. Polymerization process occurs in the presence of target molecules which are later removed during purification process leaving behind target binding cavities. This results in the formation of functionalized Au-MIP as depicted in Figure 1. Thickness of the polymer coating has been estimated as ca. 10nm based on the difference between DLS and LSPR readings and confirmed as ca. 5nm based on TEM imagery (Figure 2) but this properties can be controlled by changing reaction conditions – see section 3.2. Yield of Au- MIPs was calculated by a comparison of integrated spectra's of Au^{3+} ions (present in a raw material, $AuHClO_4$ solution) and of fully formed Au- MIPs after the purification process (Appendix) and it was calculated as 71% (Appendix Section 1, Figure S1).

Acetylacetonate is a well-researched ligand and its use in coordination chemistry of gold has previously been reported[42]. Notably, Zhang and co-authors reported formation of AuNPs using acetylacetone followed by UV-irradiation[43]. In the reaction developed by our group, acetylacetone plays dual role. Firstly, it is a reducing agent which transforms Au^{3+} ions into AuNPs, secondly it is a reagent in Michael addition type reaction where it forms carbon-carbon bonds with acrylamide monomers. Similar work has been reported before[44]. We postulate that the presence of acetylacetone in the polymerization process not only results in a formation of stable (i.e., non-precipitating) and size-homogeneous functionalized AuNPs but also paves the way for gold-catalysed

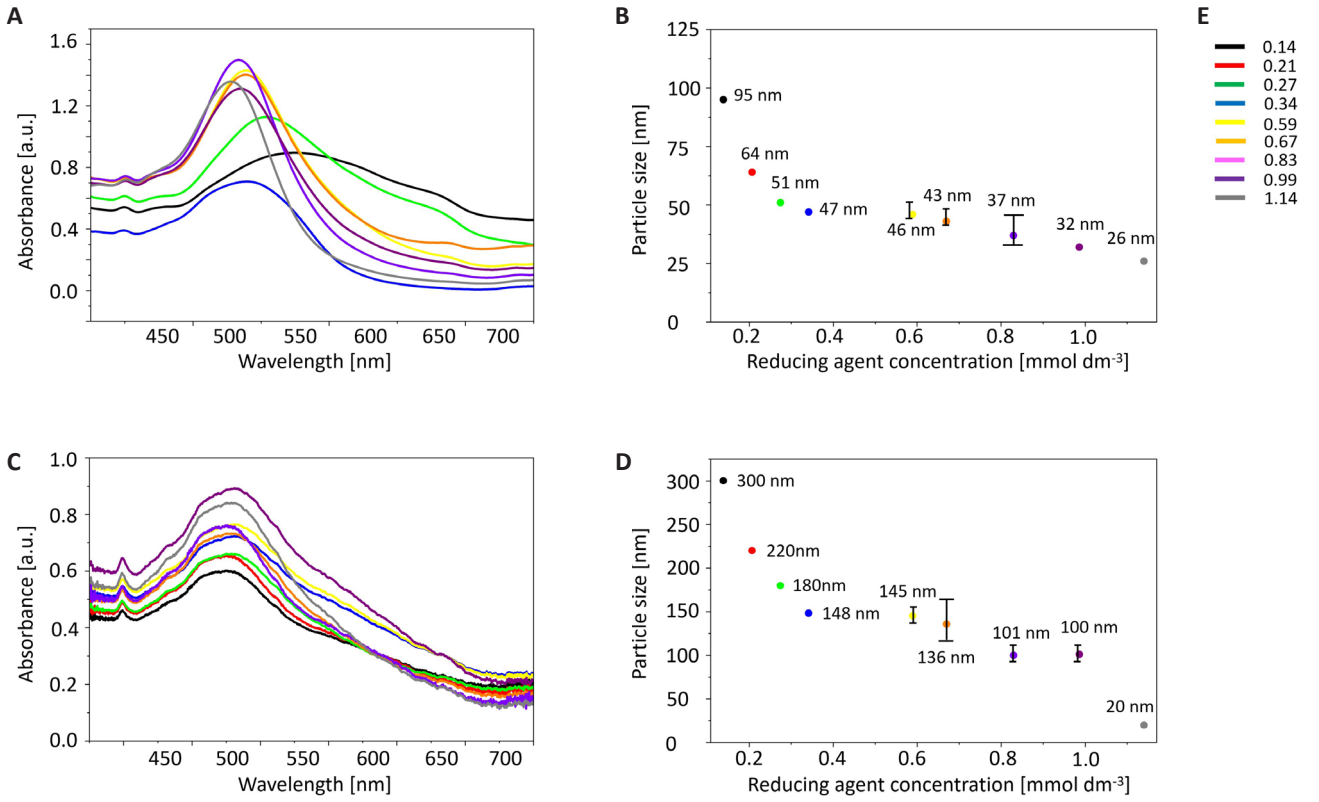


Figure 3. LSPR (left panel) and Particle Size/ketone Concentration Correlation of Bare AuNPs (A and B) and Au-core MIPs (C and D) Prepared using acetylacetone/acetone 2:1 Mixture as Gold Reducing Agent. Total particle size was determined using DLS. Figure 3E depicts concentration of reducing agent used (mmol/dm^3).

acetalization. Such reactions catalysed by gold salts have been reported before[45] as being acid catalysed[46]. Functionalization of pre-synthesized AuNPs with acrylamide has been reported previously[47,48] but not as a one-pot reaction combining nanoparticle formation and Michael's addition forming a polymer shell around AuNPs as it is in our case. Acetylacetone is not miscible with water and addition of acetone which is fully miscible with water was found to accelerate the formation of nanoparticles and improve their size/shape homogeneity.

3.2 Physical Properties of Composite Nanoparticles

Hence the overall reaction mechanism can be postulated as follows: carbonyl group rich acetone/acetylacetone mixture reduces Au^{3+} ions to Au^0 forming AuNPs. As soon as the first AuNPs emerge, their surfaces serve as catalytic sites for H_2O_2 decomposition yielding *OH radicals. This initiates radical polymerization of polyacrylamide at AuNPs surfaces. Simultaneously, both ketones undergo Michael addition catalysed by the presence of acrylic and auric acids, forming carbon-carbon bonds with acrylamides and thus become incorporated into the expanding polymer shell. The TEM image shows the Au-core MIP nanoparticles with average diameter of 20±1nm (Figure 2B). The DLS data shows aggregation effect for particles in solution with maximum size of aggregates at 300±50nm (see Figure 3D). Formation of polyacrylic shell over the in-situ formed gold nanoparticles has been confirmed by FTIR (see Figure 2A). Peaks at 1,200 and 3,400cm^{-1} confirm the presence of amide's carbonyl group and N-H groups respectively.

Notably, the size of composite gold-MIP nanoparticles produced using our method can be tightly controlled by varying the concentration of the reducing agent (RA). This is particularly important for LSPR effects that depend on the size of gold cores. Our novel methodology results in a formation of highly homogeneous AuNPs with easily controllable size (see Figure 3A and 3B). We have extended this methodology to the polymerization process which allowed us to control Au- MIPs polymer content (i.e., thickness of the polymer shell vs. gold core). It can be noted from Figure 3C and 3D that the general trend is that smaller concentration of RA lead to the formation of small number of larger AuNPs which are subsequently coated in the polymer. Slower reaction pace allows for extensive cross-linking resulting in formation of large AuMIP clusters ca. 300nm in diameter with high polymer loading. This is confirmed by the fact that Au-MIP LSPR wavelength shows little change (Figure 3C) whereas size of Au-MIP increases up to 300nm. (Figure 3D) If size of AuNP were to increase proportionally to the thickness of polymer shell, this should produce significant right LSPR shift. We consider this finding to be an advantage because thicker polymer shell can contain more binding cavities for the target molecule thus improving the performance of our sensors.

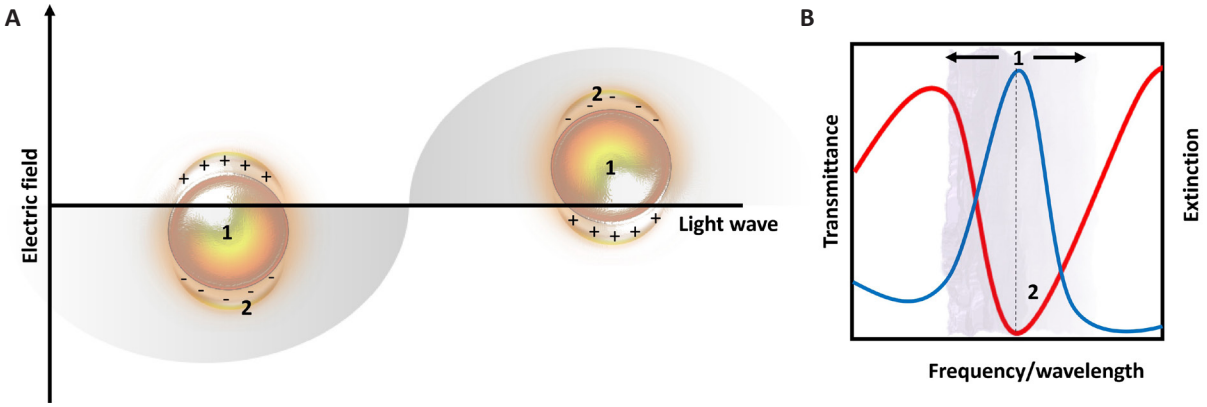


Figure 4. Principles of LSPR – Nanostructures of Noble Metals when Exposed to Incident Light at Specific Resonance Wavelengths Produce Strong Absorbance and Scattering. A: Oscillation of free electrons present in AuNPs; B: Position of an LSPR peak with respect to transmittance and extinction frequencies. This scattering originates from plasmon oscillation caused by the displacement of the conduction electron charge cloud. Frequency and intensity of this oscillation are metal specific and strongly dependent on the size, shape and environment of the noble metal nanostructures[50].

3.3 Composite Nanoparticles as Sensors for Explosives Detection

In this work Au-MIPs response towards the target was recorded by LSPR. The principle of molecular LSPR sensing using Au-MIPs relies on conformational changes in polymer shell triggered by MIP interaction with target molecules. This "gate effect" produces change in refractive index and generate spectral shifts proportional to target concentration[49]. However, in the case of MIP technique the LSPR wavelength shift is proportional to target concentration only for measurements in gas environment. In the case of liquid measurements superposition in changing of MIP refractive index exists when target molecule brings water into the imprinted cavity that results in the decrease of MIP refractive index due to the swelling of the now hydrated, polymer shell. The resonant frequency shift of Au nanoparticle's electron cloud is easily measured and quantified (see Figure 4).

3.4 Detection of Explosive Analogues in Vapour Phase

3.4.1 Sensor Design

Prototype of 2-channel photometric sensor for explosives detection was developed (Figure 5). Field operation of the portable detector has been shown in Figure S4. The device provides measurements in both gas and liquid phase by utilizing Au LSPR nanochips placed into spectrophotometric cuvettes with an optical path length of 10mm. Detector is designed for quantitative determination of adsorption of the analyte molecules on the surface of the nanochip. The adsorption value is determined by the level of light absorbance in the 400-750nm wavelength range. This is achieved using selective light sources (Cree LED JB5630AWT white LED with correlated color temperature of 4,000K, 90 CRI) and radiation detectors (2 Vishay Semiconductors BPW21R silicon photodiodes with spectral bandwidth range of 420 to 675nm). The estimated noise level of photodiode is 1nV and total noise level of photometric converter is 21μV (with ADC input of 1V), which translates to the dynamic range limit of photometric converter signal due to the noise of the measuring path of ~93 dB. Noise calculations of the photo amplifier are in accordance with the recommendations[49]. The photovoltaic mode of photodiode is used, which has zero voltage potential across the photodiode. As a result, no dark current flows through the photodiode, the linearity and sensitivity are maximized, and the noise level is relatively low, which makes it well suited for precision applications. A differential measurement scheme is used, in which the intensity of the radiation flux of the light passing through the measuring channel and through the reference channel is measured. Changes in the optical density (OD) are defined as the signal difference in the two measured channels:

$$\Delta OD = lg\left(\frac{I_0}{I_m}\right) - lg\left(\frac{I_0}{I_{ref}}\right)$$

I_0 – the radiation flux of the incident light, I_{ref} – light transmitted through the reference channel, I_m – light transmitted through the measuring channel, respectively.

Kinetic dependences of absorbance shift for mentioned Au LSPR nanochips upon exposure to o-nitrophenol vapor from different amounts of the explosive analogue are shown in Figure 6. Absorbance response exhibits expressed concentration-dependent behavior and signal-to-noise ratio sufficient for the detection of explosive analogues in vapour phase at femtogram levels (10fg o-nitrophenol in 4.5cm^3 volume) with a response time up to 5 min leading to optical absorbance response up to $7 \cdot 10^{-4}$ upon detection. 2-channel photometric sensor with Au LSPR nanochips coated with o-nitrophenol imprinted Au-MIPs exhibits baseline drift of $5 \cdot 10^{-6}$min^{-1} and noise level of $1.5 \cdot 10^{-5}$, resulting in a signal-to-noise ratio of 47 for 5min exposure to 10fg o-nitrophenol, which confirms that limit of detection (based on a signal-to-noise ratio of 3) and limit of quantitation (based on a signal-to-noise ratio of 10) of the developed sensor are indeed in the femtogram range.

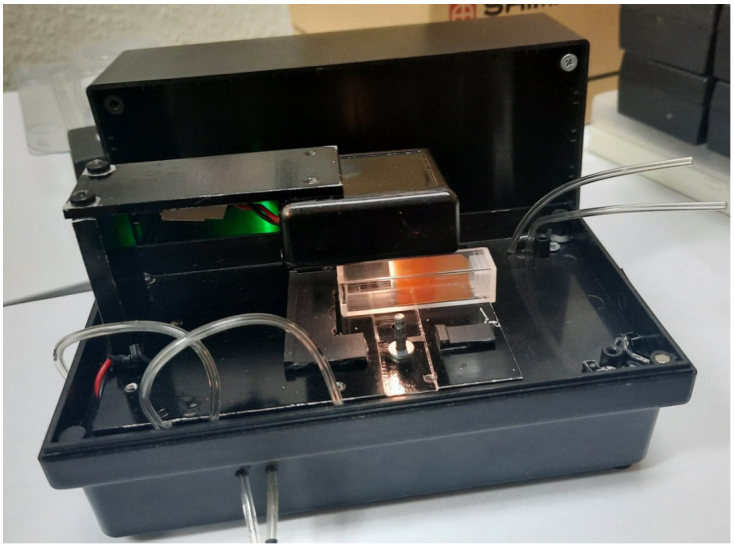


Figure 5. Prototype of 2-channel Photometric Sensor for Explosives Detection.

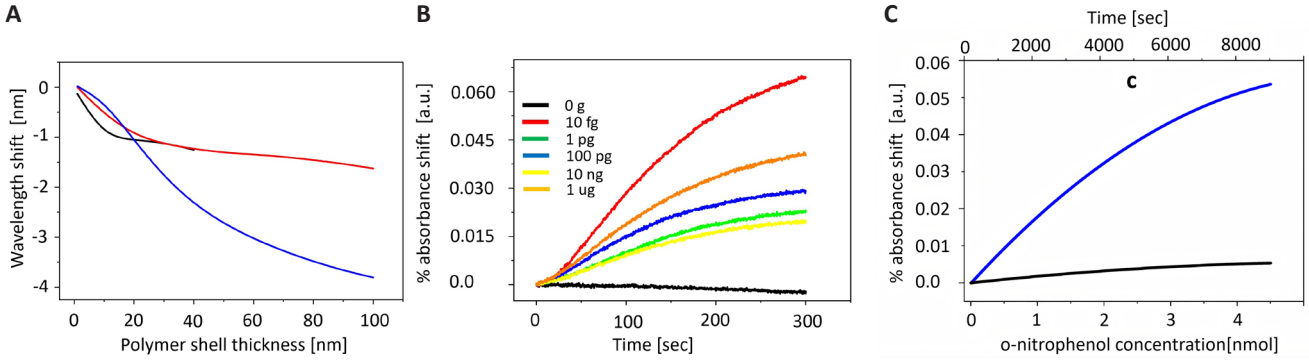


Figure 6. Detection of An Explosive Analogue in Vapor and Liquid Phases Using AuMIPs. A: Simulated LSPR shift in the light extinction spectrum of Au-MIPs upon the detection of o-nitrophenol for different gold nanoparticle size and Au-MIP polymer shell thickness. Fraction of imprinted sites occupied with o-nitrophenol molecules after detection was equal to (a)10%, (b)50%, (c)100%. Au-MIP shell imprinted sites volume fraction (porosity) was fixed at 5% and MIP shell swelling (by volume) of 10% was assumed after interaction with o-nitrophenol molecules. B: Kinetic dependences of absorbance for Au LSPR nanochip coated with o-nitrophenol imprinted Au-MIPs upon exposure to o-nitrophenol vapor from different amounts of the explosive analogue. C: Kinetic dependences of absorbance for Au LSPR nanochip coated with o-nitrophenol imprinted Au-MIPs (blue line) and Au-NIPs (black line) upon exposure to increasing concentration of o-nitrophenol dissolved in H_2O.

Cumulative dose-response dependences for different Au LSPR nanochips upon exposure to o-nitrophenol vapor from different amounts of the explosive analogue are shown in Figure S3. It is evident that selective detection of o-nitrophenol results in cumulative responses that are considerably larger than the ones observed upon the non-selective detection in the whole range of studied analyte concentrations, confirming the efficiency of Au-MIP approach for explosive analogue vapor detection. Influence of the polymer shell thickness and overall nanoparticle size on the magnitude of the LSPR signal has also been investigated. It has been found that the optimum signal-to-noise ratio was recorded for nanoparticles 100nm in diameter with 100nm thick polymer coating (see Figure 6A).

3.4.2 Detection of Explosive Analogues in the Liquid Phase

The detection of o-nitrophenol in a liquid phase was conducted as follows. Au-MIPs imprinted for o-nitrophenol were immobilized on the surface of Au LSPR nanochips (arrays of Au nanostructures on glass slides-Figure S1) via 1-Ethyl-3-(3-dimethylaminopropyl) carbodiimide (EDC) and *N*-Hydroxy succinimide (NHS) coupling (Figure S5). Nanochips were then placed in a UV cuvettes filled with deionized water. Cuvettes were placed in the spectroscopic chamber of Nano SPR-103 spectrometer) connected to a syringe pump (Oxford Instruments, UK). While continuous measurements of the LSPR spectra were being recorded by the spectrometer, pump was used to inject 10mM aqueous solution of o-nitrophenol into the cuvette until the concentration of 4.5nM has been reached over the period of 8,000 sec (i.e., 562.5fM sec^{-1}) Target injection rate in liquid phase study has been adjusted considering viscosity of water (54.7 larger than viscosity of air). The results of target detection in liquid phase are shown in Figure 6C. AuNP-MIPs imprinted o-nitrophenol (analogue for trinitrotoluene) were tested versus increased concentrations of the target molecules with results shown above in Figure 6. MIPs imprinted o-nitrophenol displayed

logarithmic increase in LSPR absorbance in both vapour (Figure 6B) and liquid (Figure 6C) phase detection.

4 CONCLUSION

Novel sensors for explosives detection have been reported. At the core of the sensor are composite Au-MIP nanoparticles which are formed by one-pot synthesis combining AuNP formation, radical polymerization and Michael addition. When applied as sensors, these nanoparticles display excellent sensitivity in the detection of explosives analogues at femtomolar concentration. Development of a portable detector capable of detection of femtogram concentrations of TNT analogue (o-nitrophenol) in both vapour and liquid phases has also been reported. Prototyping work described here paves the way for practical applications of MIPs based sensing in explosives detection.

Acknowledgements

Authors acknowledge funding from North Atlantic Treaty Organization (NATO), project number G5361.

Conflicts of Interest

The authors declared no conflict of interest.

Data Availability

The data that support the findings of this study are available from the corresponding author upon reasonable request.

Author Contribution

Whitcombe M, Piletska E, Garcia Cruz A, Lopatynskyi A, Lytvyn V, Chegel V and Zaleski C conducted laboratory experiments. Piletsky S and Chegel V concepted and designed the research; Lopatynskyi A, Lytvyn V, Chegel V, Zaleski C analyzed and interpretated the results; Zaleski C drafted the manuscript; All authors have read and approved the final version of the manuscript.

Abbreviation List

AuMIP, Gold core molecularly imprinted polymer
AuNP, Gold nanoparticles
DLS, Dynamic light scattering
FTIR, Fourier transformation infra-red spectroscopy
LODs, Limits-of-detection
LSPR, Localized surface plasmon resonance
MIPs, Molecularly Imprinted Polymers
TEM, Transmission electron microscopy

References

[1] Barnawi A, Kumar K, Alzahrani B et al. A comprehensive review on landmine detection using deep learning techniques in 5G environment: open issues and challenges. *Neural Comput Appl*, 2022; 34: 21657-21676.[DOI]

[2] Karnik S, Prabhu R. Chemical detection of explosives in soil for locating buried landmine. Proc SPIE, 2021; 11869: 1186902.[DOI]

[3] Bausinger T, Bonnaire E, Preuß J. Exposure assessment of a burning ground for chemical ammunition on the Great War battlefields of Verdun. *Sci Total Environ*, 2007; 382: 259-271.[DOI]

[4] Wasilewski T, Gębicki J. Emerging strategies for enhancing detection of explosives by artificial olfaction. *Microchem J*, 2021; 164: 106025.[DOI]

[5] Kagan A. Counterterrorist detection techniques of explosives by vapor sensors (handheld). In: Kagan A, Oxley JC, editors. Counterterrorist Detection Techniques of Explosives. 2nd ed. Elsevier: Amsterdam, *Netherlands*, 2022: 235-251.[DOI]

[6] 908 Devices. MX908 Handheld Explosives and Narcotics Detector. 908 Devices. Available at:[Web]

[7] Smiths Detection. LCD 4.1 Explosives and Narcotics Trace Detector. Smiths Detection. Available at:[Web]

[8] GS Automatic. Explosive & Narcotics Detector Using Fluorescent Polymer Technology | GS808. Available at:[Web]

[9] Nuctech. Nuctech Explosives Detection Systems. Nuctech. Available at:[Web]

[10] Safeagle. Safeagle Explosives and Narcotics Trace Detectors. Safeagle. Available at:[Web]

[11] Rapiscan Systems. MobileTrace Explosives and Narcotics Trace Detector. Rapiscan Systems. Available at:[Web]

[12] Bruker. RoadRunner Handheld Explosives and Narcotics Trace Detector. Bruker. Available at:[Web]

[13] Procek M, Stolarczyk A, Pustelny T et al. A Study of a QCM Sensor Based on TiO2 Nanostructures for the Detection of NO2 and Explosives Vapours in Air. *Sensors*, 2015; 15: 9563-9581.[DOI]

[14] Eslami MR, Alizadeh N. Ultrasensitive and selective QCM sensor for detection of trace amounts of nitroexplosive vapors in ambient air based on polypyrrole—Bromophenol blue nanostructure. *Sens Actuators B Chem*, 2019; 278: 55-63.[DOI]

[15] MS Tech. MS Tech Explosives Detection Solutions. MS Tech. Available at:[Web]

[16] Majumder S, Murali K, Gorthi SS et al. Standoff Detection of Explosives Using Compressive-Sensing-Enabled Raman Spectral Imaging. *IEEE Sens J*, 2024; 24: 28094-28099.[DOI]

[17] Huang Y, Liu Z, Zhang Y et al. Detection of Buried Explosives Using a Surface-Enhanced Raman Scattering (SERS) Substrate Tailored for Miniaturized Spectrometers. *ACS Sens*, 2020; 5: 2933-2939.[DOI]

[18] Sen Bishwas M, Malik M, Poddar P. Raman spectroscopy-based sensitive, fast and reversible vapour phase detection of explosives adsorbed on metal–organic frameworks UiO-67. *New J Chem*, 2021; 45: 7145-7153.[DOI]

[19] Verma AK, Soni RK. Ultrasensitive surface-enhanced Raman spectroscopy detection of explosive molecules with multibranched silver nanostructures. *J Raman Spectrosc*, 2022; 53: 694-708.[DOI]

[20] Department of Homeland Security. Explosives Trace Detectors (ETDs) Market Survey Report. DHS, 2021.

[21] DetectaChem. DetectaChem Explosives and Narcotics Detection Products. DetectaChem. Available at:[Web]

[22] SERSTECH. Serstech ARX Handheld Raman Spectrometer. Serstech. Available at:[Web]

[23] Li L, Wang Y, Zhang H et al. Application of fluorescence sensing technology in trace detection of explosives. *Dyes Pigm*, 2023; 220: 111651.[DOI]

[24] Teledyne FLIR. Fido X4 Explosives Trace Detector. Teledyne FLIR. Available at:[Web]

[25] Hewei Defense. Hewei Defense Explosives Detection Solutions. Hewei Defense. Available at:[Web]

[26] Korposh S, James SW, Lee SW et al. Selective vancomycin detection using optical fibre long period gratings functionalised with

molecularly imprinted polymer nanoparticles. *Analyst*, 2014; 139: 2229-2236.[DOI]

[27] Mahajan R, Rouhi M, Tavares A et al. Highly Efficient Synthesis and Assay of Protein-Imprinted Nanogels by Using Magnetic Templates. *Angew Chem Int Ed*, 2019; 58: 727-730.[DOI]

[28] Sergeyeva T, Yarynka D, Piletska E et al. Fluorescent sensor systems based on nanostructured polymeric membranes for selective recognition of Aflatoxin B1. *Talanta*, 2017; 175: 101-107.[DOI]

[29] Canfarotta F, Piletsky SA. Engineered magnetic nanoparticles for biomedical applications. *Adv Healthc Mater*, 2014; 3: 160-175.[DOI]

[30] Cardoso AR, Tavares APM, Sales MGF. In-situ generated molecularly imprinted material for chloramphenicol electrochemical sensing in waters down to the nanomolar level. *Sens Actuators B Chem*, 2018; 256: 420-428.[DOI]

[31] Anirudhan TS, Athira VS, Chithra Sekhar V. Electrochemical sensing and nano molar level detection of Bisphenol-A with molecularly imprinted polymer tailored on multiwalled carbon nanotubes. *Polymer*, 2018; 146: 312-320.[DOI]

[32] Mehmandoust M, Soylak M, Erk N. Innovative molecularly imprinted electrochemical sensor for the nanomolar detection of Tenofovir as an anti-HIV drug. *Talanta*, 2023; 253: 123991.[DOI]

[33] Stephen AN, Chianella I, Piletska E et al. Rapid sub-nanomolar protein determination in serum using electropolymerized molecularly imprinted polymers (E-MIPs). *Analyst*, 2023; 148: 5476-5485.[DOI]

[34] Stringer RC, Gangopadhyay S, Grant SA. Detection of Nitroaromatic Explosives Using a Fluorescent-Labeled Imprinted Polymer. *Anal Chem*, 2010; 82: 4015-4019.[DOI]

[35] Chegel V, Nazarenko V, Lytvyn P et al. Localized surface plasmon resonance nanochips with molecularly imprinted polymer coating for explosives sensing. *Semicond Phys Quantum Electron Optoelectron*, 2020; 23: 431-436.[DOI]

[36] Riskin M, Ben-Amram Y, Tel-Vered R et al. Molecularly imprinted Au nanoparticles composites on Au surfaces for the surface plasmon resonance detection of pentaerythritol tetranitrate, nitroglycerin, and ethylene glycol dinitrate. *Anal Chem*, 2011; 83: 3082-3088.[DOI]

[37] Lin Y, Ren J, Qu X. Catalytically Active Nanomaterials: A Promising Candidate for Artificial Enzymes. *Acc Chem Res*, 2014; 47: 1097-1105.[DOI]

[38] Fang Q, Zhou X, Deng W et al. In situ redox-oxidation polymerization for magnetic core-shell nanostructure with polydopamine-encapsulated-Au hybrid shell. *J Hazard Mater*, 2019; 367: 15-25.[DOI]

[39] Kim HM, Jin SM, Lee SK et al. Detection of Biomolecular Binding Through Enhancement of Localized Surface Plasmon Resonance (LSPR) by Gold Nanoparticles. *Sensors*, 2009; 9: 2334-2344.[DOI]

[40] Song Y, Xu Z, Wang Q et al. LSPR-enhanced photonic crystal allows ultrasensitive and label-free detection of hazardous chemicals. *Sens Actuators B Chem*, 2020; 310: 127671.[DOI]

[41] Poma A, Guerreiro A, Whitcombe MJ et al. Solid-Phase Synthesis of Molecularly Imprinted Polymer Nanoparticles with a Reusable Template–"Plastic Antibodies". *Adv Funct Mater,* 2013; 23: 2821-2827.[DOI]

[42] Vicente J, Chicote MT. The 'acac method' for the synthesis of coordination and organometallic compounds: synthesis of gold complexes. *Coord Chem Rev*, 1999; 193-195: 1143-1161.[DOI]

[43] Zhang L, Wang J, Liu X et al. An all-in-one approach for synthesis and functionalization of nano colloidal gold with acetylacetone. *Nanotechnology*, 2022; 33: 075605.[DOI]

[44] Deuri S, Phukan P. A stepwise mechanism for the uncatalyzed michael addition of acetylacetone to methyl vinyl ketone. *Int J Quantum Chem*, 2012; 112: 801-808.[DOI]

[45] Belot S, Vogt KA, Besnard C et al. Enantioselective One-Pot Organocatalytic Michael Addition/Gold-Catalyzed Tandem Acetalization/Cyclization. *Angew Chem Int Ed*, 2009; 48: 8923-8926.[DOI]

[46] Dorel R, Echavarren AM. Gold(I)-Catalyzed Activation of Alkynes for the Construction of Molecular Complexity. *Chem Rev*, 2015; 115: 9028-9072.[DOI]

[47] Nie L, Zhang Q, Hu L et al. Fabrication of micropatterned gold nanoparticles on graphene oxide nanosheet via thiol-Michael addition click chemistry. *Mater Lett*, 2020; 261: 127014.[DOI]

[48] Lu X, Zhang H, Li Y et al. Light-Controlled Shrinkage of Large-Area Gold Nanoparticle Monolayer Film for Tunable SERS Activity. *Chem Mater*, 2018; 30: 1989-1997.[DOI]

[49] Hwang RB. A theoretical design of evanescent wave biosensors based on gate-controlled graphene surface plasmon resonance. *Sci Rep*, 2021; 11: 1999.[DOI]

[50] Hutter E, Fendler JH. Exploitation of Localized Surface Plasmon Resonance. *Adv Mater*, 2004; 16: 1685-1706.[DOI]